Tellus (1998), 50A, 525–533
Printed in UK – all rights reserved

TELLUS
ISSN 0280–6509

The unexplained solar absorption and atmospheric H_2O: a direct test using clear-sky data

By WILLIAM C. CONANT[1], ANDREW M. VOGELMANN and V. RAMANATHAN,
Center for Clouds, Chemistry and Climate and Center for Atmospheric Sciences, Scripps Institution of Oceanography, University of California at San Diego, CA, USA

(Manuscript received 4 August 1997; in final form 6 March 1998)

ABSTRACT

This paper is motivated by several recent studies that have shown that observations of atmospheric solar absorption systematically and significantly exceed model estimates. This paper tests whether uncertainties in the physics of water vapor absorption in clear skies are directly responsible for this unexplained excess absorption. Radiative transfer calculations of clear-sky solar fluxes are compared to measurements in the tropical Pacific at the surface and the tropopause. We find that the atmospheric absorption in excess of that predicted by radiative transfer models, if it exists, is less than the experimental uncertainty of 7 W m^{-2} (diurnally averaged). Furthermore, the difference between observed and modeled absorption is essentially independent of water vapor amounts between 35 and 51 kg m^{-2}. A more direct test of the accuracy of modeled water vapor absorption is conducted with two independent multi-spectral radiometers at the Atmospheric Radiation Measurement site in Oklahoma, each providing over 16 000 surface measurements of direct solar radiation in the 0.94 μm region. These spectral data confirm state-of-the-art radiation model computations of water vapor line absorption to within 5% for the wavelength region tested. The model-observation agreement for both tropical and Oklahoma data strongly suggests that uncertainties in the physics of water vapor absorption in clear skies are not a source for any significant excess solar absorption, thus narrowing the search to other atmospheric constituents or water vapor in cloudy skies.

1. Introduction

Observational estimates of atmospheric solar absorption are systematically larger than model estimates by as much as 15 to 30 W m^{-2} globally (and diurnally) averaged (Ohmura and Gilgen, 1993; Wild et al., 1995; Cess et al., 1995; Ramanathan et al., 1995; Pilewskie and Valero, 1995; Arking, 1996). Currently there is a debate as to whether this unexplained excess absorption (observed minus modeled) is in clear skies (Wild et al., 1995; Arking, 1996; Charlock and Alberta, 1996) or cloudy skies (Cess et al., 1995; Ramanathan et al., 1995; Pilewskie and Valero, 1995), or is an artifact of experimental uncertainties (Stephens, 1996). Arking (1996) estimates a global excess absorption of 25 to 30 W m^{-2} which he states is correlated to column H_2O* in clear skies. The 40–45 W m^{-2} H_2O absorption computed by models (Kiehl and Trenberth, 1997; Liou, 1992) has to be in error by more than 50% for H_2O to be the sole source of the unexplained absorption. The conclusion that model errors increase with clear-sky H_2O content was derived

[1] Corresponding author: Center for Clouds, Chemistry and Climate, Scripps Institution of Oceanography, University of California, San Diego, La Jolla, CA 92093–0221, USA. e-mail: wconantæucsd.edu

* The term H_2O in this paper refers only to water vapor and its polymers.

from monthly-mean cloudy-sky data, from which it is difficult to isolate cause from effect. We isolate the physics of H_2O absorption by comparing state-of-the-art radiative transfer calculations to clear-sky measurements of calibrated broadband solar fluxes in the tropical Pacific and spectral direct solar radiances from a continental mid-latitude site. By using only clear-sky data, we do not test the absorption by cloudy-sky H_2O where uncertainties in H_2O physics (e.g., continuum/polymer absorption or the H_2O-cloud distribution) may be enhanced with respect to sub-saturated, clear-sky conditions.

2. Tropical broadband comparison

Calibrated measurements of broadband (0.3–2.8 μm) solar radiation taken during the Central Equatorial Pacific Experiment (CEPEX) in March, 1993 from ship and aircraft provide the ideal data for testing model H_2O absorption because: (1) the 10-s sampling allows clear skies to be isolated from cloudy skies; (2) the column H_2O in this region is 35–51 kg m^{-2}, where Arking (1996) finds the largest model errors; (3) the effect of absorbing continental aerosols will be minimal because the data used here are from the central equatorial Pacific ocean at 2°S (between 150°E and 170°W), several thousand kilometers from any major industrialized regions or biomass burning sites. The data and models summarized below are described in full detail elsewhere (Conant, 1996; Conant et al., 1997).

The University of Southern California Research Vessel J. Vickers carried a gimbaled upward-facing pyranometer on its near-equatorial cruise between 165°E and 155°W. The pyranometer was calibrated versus a primary-standard radiometer before and after the CEPEX cruise yielding an accuracy better than 2%. Likewise, the low-flying NOAA P-3 aircraft carried identical upward- and downward-facing pyranometers calibrated before each flight yielding accuracies within 10 W m^{-2}. The clear-sky surface irradiance measured by the ship and aircraft agree within 0.3% when binned by solar zenith angle and averaged. Multiplying the measured downward irradiance by one minus the observed surface albedo yields the net solar radiation absorbed by the ocean. The diurnally averaged clear-sky net surface solar radiation estimated from the measurements is 311 W m^{-2} with an experimental uncertainty of 5 W m^{-2} (1.7%).

At the tropopause, net solar radiation was measured by bolometric radiometers accurate to within 1% flown aboard the NASA ER-2 aircraft. These instruments measured virtually the same spectral region as the surface pyranometers. The clear-sky albedo determined by the tropopause measurements (after accounting for stratospheric effects) agreed with historical pixel-scale Earth Radiation Budget Experiment (ERBE) albedos. The satellite data were also used to quantify the variability of the clear-sky albedo. The diurnally averaged net solar radiation absorbed by the clear-sky tropical ocean-atmosphere column is 400 ± 4.5 W m^{-2}.

The broadband atmospheric solar absorption of 89 ± 7 W m^{-2} (diurnal average) is obtained by subtracting the clear-sky net surface solar radiation from that obtained from the tropopause and satellite observations. The 7 W m^{-2} uncertainty includes effects from the observed variability, instrumental accuracy and spectral overlap between the surface and top-of-atmosphere (TOA) platforms. Note that the above values are diurnal averages — solar fluxes and uncertainties are typically larger for instantaneous measurements.

Two radiative transfer models determine the surface and atmospheric solar absorption for comparison with the observations. Each model takes as input column H_2O measured by Vaisala sondes launched from the Vickers every 6 hours. The observed solar zenith angle dependent clear-sky albedo is used as a constraint on the models.

The first model solves the radiative transfer equation using the discrete ordinates method in 38 spectral regions from 0.2 to 4.0 μm. As input, the model uses observed profiles of H_2O and O_3, stratospheric aerosol properties and solar zenith angle dependent ocean surface albedos. (The model stratospheric aerosol includes a remnant from the Pinatubo eruption of 1991, which was measured during CEPEX by instruments aboard the ER-2.) To ensure that the model results bound the observed variability in clear-sky albedo, two runs of the model with differing aerosol optical depths (0.03 to 0.24) were performed. This yielded a 1.5 W m^{-2} uncertainty in diurnally averaged atmospheric absorption due to uncertainties in boundary layer aerosol optical depth.

The second model, the Li et al. (1993) transfer function, parametrically determines atmospheric and surface solar absorption based on a climatological sub-arctic atmosphere and observed column H_2O and clear-sky albedo. Small modifications were necessary to account for a tropical O_3 profile and the presence of the Pinatubo aerosol. In contrast to the conservative maritime aerosol used by the discrete ordinates model, the Li et al. (1993) model uses an absorptive Arctic Haze aerosol (Blanchet and List, 1983) of fixed 0.05 optical thickness.

The modified Li et al. (1993) model atmosphere is 6.5 W m^{-2} more absorptive than the discrete ordinates model. Part, but not all, of this difference can be attributed to the more absorptive Arctic Haze aerosol. By using these two models, we bracket reasonable uncertainties in inter-model differences and aerosol absorption. For the purpose of model-observation comparison, the model results are averaged yielding a 90 W m^{-2} atmospheric absorption. An uncertainty of 5.5 W m^{-2} is derived from an rms combination of the model discrepancy and the models' sensitivities to the observed variabilities in constraining parameters (i.e. H_2O and albedo).

Fig. 1 shows that the diurnally averaged observed atmospheric absorption agrees with the models within the experimental uncertainty of 7 W m^{-2}. In this region of high column H_2O (35 to 51 kg m^{-2} compared to the global average of 25 kg m^{-2}) and high TOA insolation (441 W m^{-2} versus 340 W m^{-2} globally), we expect any model-observation discrepancy in clear-sky H_2O absorption to be large compared to the global average discrepancy. That the errors in this moist region are constrained to be within 7 W m^{-2} is inconsistent with the hypothesis that H_2O in clear skies is absorbing 25 W m^{-2} globally in excess of that predicted by models.

Two other studies confirm that models and observations agree on the solar energy absorbed by the tropical Pacific ocean, suggesting that the atmospheric absorption is well modeled. Waliser et al. (1996) find that buoy measurements of net surface radiation of 310–315 W m^{-2} agree well with the Li et al. (1993) transfer function for the tropical Western Pacific during the Tropical Ocean Global Atmosphere's (TOGA) Coupled Ocean Atmosphere Response Experiment (COARE), carried out between October 1992 and March 1993. This result was confirmed by Chou and Zhao (1997) using TOGA COARE island station measurements of direct and diffuse surface radiation and an 11-band delta-Eddington model.

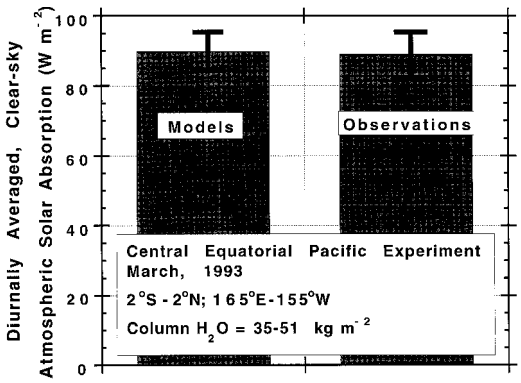

Fig. 1. Diurnal average solar radiation in W m^{-2} absorbed by the clear-sky atmosphere during CEPEX. The model estimate (left) is obtained by averaging results from two clear-sky models, each constrained by the observed column H_2O and TOA albedo. Uncertainty in the model result, shown as a range bar, is estimated from the difference between the models and the variability in the H_2O and albedo measurements used as model input. The observed estimate (right) is from ship, aircraft and satellite data. Uncertainty in the observed estimate is derived from instrumental accuracies and variability in the data. The data and models are thoroughly described in Conant et al. (1997).

It might be argued that a model error in H_2O absorption is compensated for in the above analysis by non-H_2O errors elsewhere in the broad solar spectrum. We test this using unaveraged CEPEX data by seeing if there is any correlation between H_2O and model-observation differences. Fig. 2a plots the percent difference between the modified Li et al. (1993) model using coincident H_2O profiles as input and the instantaneous measured surface irradiance versus H_2O. Aerosol in the model is fixed, and thus will not correlate to H_2O column. No trend is observed linking model errors to H_2O column, we thus conclude that there are no significant H_2O related biases in the clear-sky model.

This point is illustrated differently in Fig. 2b in which the modeled atmospheric absorption is plotted directly versus observations derived from instantaneous surface and TOA measurements. No appreciable unmodeled atmospheric absorption is apparent, which would be revealed as

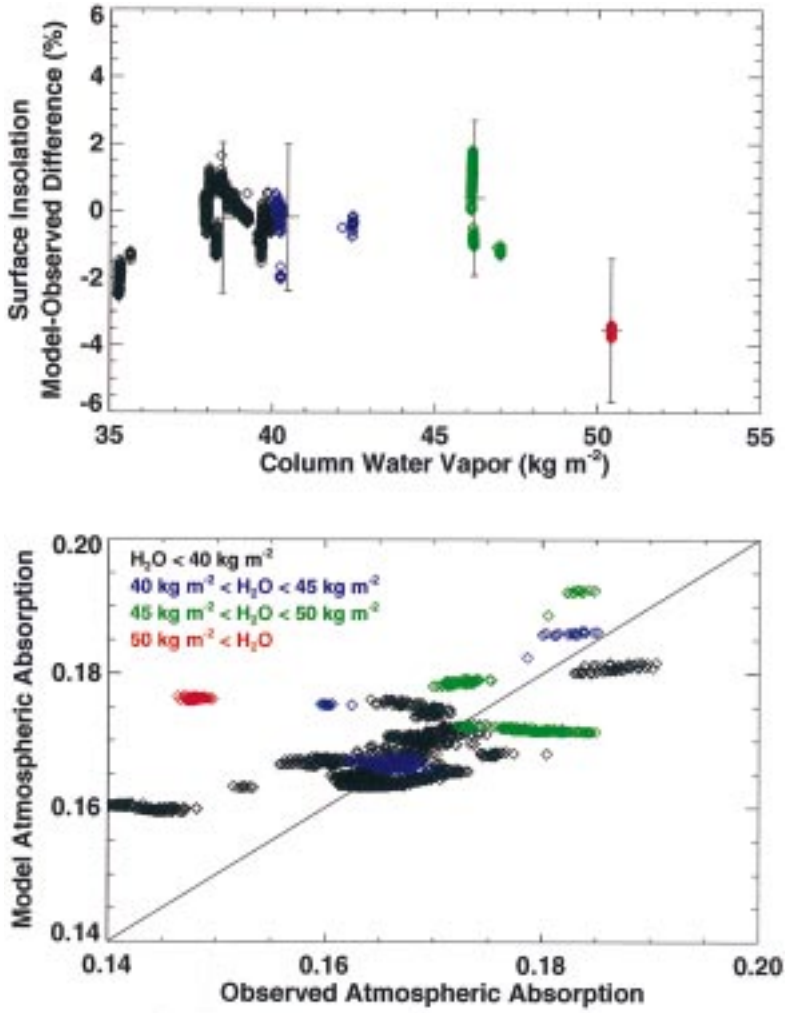

Fig. 2. (A) Broadband model minus instantaneous CEPEX measurements of atmospheric transmission (expressed as a fraction of the TOA insolation) plotted vs. column H_2O. A positive slope would have indicated an unmodeled H_2O absorption. The experimental uncertainty for each column H_2O binned average is shown as a range bar. (B) model versus observed instantaneous atmospheric absorption. The lower right of the plot would indicate an unmodeled atmospheric absorption. Variability within a single H_2O bin is due to changes in solar zenith angle, cloud contamination and a mismatch between radiation and H_2O sampling periods.

points in the lower right of the plot. Data in Fig. 2b are color coded by column H_2O amount. There is no trend linking increased unmodeled absorption with increased H_2O. The points of highest atmospheric absorption within an H_2O bin correspond to slant zenith angles, and the model represents these data well. There is significant high-frequency noise at overhead sun angles (perhaps due to side reflections from clouds not screened by the clear-sky criteria) which prevents a meaningful trend analysis versus solar zenith angle. Regardless, even the maximum noise of .03 is not sufficient to mask a $\sim$50% uncertainty in H_2O absorption.

In summary, the unaveraged CEPEX data show that the model $-$ observation difference in neither the surface insolation (Fig. 2a) nor the atmospheric absorption (Fig. 2b) is correlated to H_2O amounts

ranging between 35 and 51 kg m^{-2} where Arking (1996) finds a significant correlation using monthly-averaged, cloudy-sky data. We thus conclude that Arking's unmodeled absorption is not caused by uncertainties in the absorption by sub-saturated, clear-sky H_2O.

3. 0.94 μm H_2O absorption

The tropical broadband data are useful to identify any gross errors in the clear-sky atmospheric absorption, but narrowband measurements are necessary to validate the physics of H_2O absorption present in current state-of-the-art model calculations. The Atmospheric Radiation Measurement's (ARM) Enhanced Shortwave Experiment (ARESE) provides spectral solar radiances at 0.94 μm and coincident vertical profiles of H_2O. ARESE was conducted from September 21 to November 1, 1995 at the Southern Great Plains ARM site near Lamont, Oklahoma (Valero et al., 1995). Two Multi-Filter Rotating Shadowband Radiometers (MFRSRs) of the same make measured narrowband direct solar radiation centered at 0.94 μm and five other visible and near-infrared regions (0.415 μm, 0.495 μm, 0.610 μm, 0.665 μm, and 0.862 μm; Harrison et al., 1994). Each radiometer has a built-in arm that rotates through the sensor's field-of-view at 20 second intervals allowing the partitioning of the solar irradiance between the direct solar beam and the diffuse sky radiation. The two MFRSRs, located within 10 meters of one another, are from the Solar and Infrared Observing System (SIROS) and the Baseline Surface Radiation Network (BSRN). The filter for each of the six channels ($n=1$ ... 6) has a spectral response function, $f_n(\lambda)$, with a width of 0.01 μm at half the maximum value of $f_n(\lambda)$. $f_6(\lambda)$, the response function for the H_2O channel, is 0 at 0.920 μm, is maximum at 0.936 μm, and reduces to 0 again at 0.948 μm.

The radiation model used for comparison takes vertical profiles of H_2O from 8-daily Vaisala balloon soundings of temperature, pressure and humidity; the Balloon Borne Sounding System (BBSS) yields total precipitable water estimates good to 5%. A two-channel, zenith-pointing Radiometrics WVR-1100 microwave radiometer (MWR) provides an independent measurement of column integrated H_2O at 20 s intervals (Liljegren, 1994). For the period considered here, the two instruments agree with a bias of 1% and a root-mean-square (rms) variance of 5%. The radiative transfer model employs the correlated-k method (Lacis and Oinas, 1991) to calculate the spectral optical depth in 100 spectral sub-bands across the 0.94 μm band. Sets of correlated-k (CK) coefficients are computed by a line-by-line model from the pressure, temperature, and H_2O profiles measured by each BBSS sounding. (H_2O retrievals from surface near-infrared measurements, e.g., Michalsky et al., 1995, in principle, do not include coincident measurements of the vertical scaling of H_2O and thus must make assumptions about the pressure and temperature line broadening.) The line-by-line model uses a Voigt lineshape and H_2O line centers, strengths and halfwidths from the HITRAN '92 database (Rothman et al., 1992). In the 0.94 μm region, the model explicitly accounts for the 1074 vibration-rotation lines of the combination bands for 4 isotopes of H_2O. Line wings 300 cm^{-1} from the line center are considered. CK calculations agree with line-by-line calculations to within 0.6%. The original versions of the CK and line-by-line codes were provided by W. Ridgeway. Details of the models and line shape effects, and additional model-data analyses can be found in Vogelmann et al., in press. Each radiative transfer calculation uses H_2O column from the 20 s MWR measurements and the corresponding CK coefficients and vertical H_2O distributions from the nearest sounding.

For comparing models with observed surface spectral radiation, we develop an analysis technique that not only separates the instrumental error, but also leads to robust conclusions that are insensitive to day-to-day or diurnal variations in H_2O profiles, aerosol, and solar zenith angle. Only clear-sky scenes are considered. Cloud screening is partially obtained from the Belfort Laser Ceilometer, a zenith viewing laser cloud profiler accurate to 7800 meters. The criteria for clear skies are that (a) the ceilometer shows no clouds for the entire sunlit day, and (b) the MFRSR direct beam measurement in the visible channels varies smoothly with the insolation at the top of the atmosphere. Data are further screened for $\mu_0 > 0.3$ (μ_0 is the cosine of the solar zenith angle), where the cosine response of the

MFRSR is well characterized. Eleven days during ARESE were found to be clear (1, 4, 6, 8, 12, 13, 15, 18, 21, and 28 October 1995). Over 16 000 collocated MFRSR and MWR measurements were available for the 11 days.

The narrowband transmission of the direct solar beam for MFRSR channel n is the ratio of the surface measurement (I_n) to that which would be made at the top of the atmosphere ($I_{0,n}$). For the 0.94 μm band (MFRSR channel 6), we have

$$\frac{I_6}{I_{0,6}} = \frac{\int f_6(\lambda) I_0(\lambda) T(\lambda) \mathrm{d}\lambda}{\int f_6(\lambda) I_0(\lambda) \mathrm{d}\lambda}, \tag{1}$$

where $I_0(\lambda)$ is the spectral solar irradiance at the top of the atmosphere as a function of wavelength λ. $T(\lambda) = \exp(-\tau(\lambda)/\mu_0)$ is the monochromatic transmission of the direct solar beam, where the vertical optical depth $\tau(\lambda)$ is defined to be $\tau(\lambda) = \tau_{\mathrm{Ray}}(\lambda) + \tau_{\mathrm{aer}}(\lambda) + \tau_{\mathrm{gas}}(\lambda)$ which is the sum of, respectively, the Rayleigh, aerosol, and gas extinction optical depths.

Since $I_0(\lambda)$, $\tau_{\mathrm{Ray}}(\lambda)$ and $\tau_{\mathrm{aer}}(\lambda)$ are effectively constant for the narrow bandwidths in question, we can approximate them with band values: $I_{0,6}$, $\tau_{\mathrm{Ray},6}$ and $\tau_{\mathrm{aer},6}$. This assumption would not be valid for H_2O. The band transmission due to H_2O, $\langle T_{\mathrm{H_2O}} \rangle_6$, is isolated by letting,

$$\frac{I_6}{I_{0,6}} = \exp\left(- \frac{\tau_{\mathrm{Ray},6} + \tau_{\mathrm{aer},6}}{\mu_0} \right) \langle T_{\mathrm{H_2O}} \rangle_6, \tag{2a}$$

where,

$$\langle T_{\mathrm{H_2O}} \rangle_6 \equiv \frac{\int f_6(\lambda) \exp\left(- \frac{\tau_{\mathrm{H_2O}}(\lambda)}{\mu_0} \right) \mathrm{d}\lambda}{\int f_6(\lambda) \mathrm{d}\lambda}. \tag{2b}$$

The observed H_2O transmission, $\langle T_{\mathrm{H_2O}} \rangle_{6,\mathrm{MFRSR}}$, is obtained by inverting eq. (2a) and substituting collocated and time dependent values for $\tau_{\mathrm{Ray},6}$ and $\tau_{\mathrm{aer},6}$. Rayleigh scattering is obtained from well known formulae (Teillet, 1990). Aerosol optical extinction will be important to estimate because it trends with H_2O for the clear-sky days selected. To avoid possible ambiguities, $\tau_{\mathrm{aer},6}$ is obtained in 3 ways: (i) assuming $\tau_{\mathrm{aer},6} = \tau_{\mathrm{aer},5}$, where eq. (2a) is used to obtain aerosol optical depth in the 0.862 μm band (channel 5) where gaseous absorption is negligible; (ii) same as (i), but we let $\tau_{\mathrm{aer},6} = C\tau_{\mathrm{aer},5}$ where C is empirically determined by fitting the observed transmission with both the model H_2O transmission and the channel 5 aerosol optical depth; and (iii) same as (ii), but we use the aerosol optical depth for channel 2 (0.495 μm) instead of 5. Channels 2 and 5 are empirically calibrated for uncertainties in the top-of-atmosphere solar radiance and the linear calibration constant by a Langley-type procedure essentially equivalent to that described in Harrison and Michalsky (1994). The use of the MFRSR to obtain atmospheric extinction formally assumes single-scattering. However, in addition to the direct solar radiation, the instrument will also measure forward-scattered radiation. This effect to first-order is implicitly accounted for by obtaining aerosol optical depth from the nearby visible channels.

$\langle T_{\mathrm{H_2O}} \rangle_{6,\mathrm{MODEL}}$, a model estimate for the channel 6 H_2O transmission, is determined by numerically integrating eq. (2b) using correlated-k calculations of $\tau_{\mathrm{H_2O}}(\lambda)$ and measured spectral responses for each of the SIROS and BSRN MFRSR filters.

A least squares linear regression technique is used to compare the model with data from the SIROS MFRSR (Fig. 3); let,

$$A_0 + A_1 \left[-\ln \langle T_{\mathrm{H_2O}} \rangle_{6,\mathrm{MFRSR}} \right] = -\ln \langle T_{\mathrm{H_2O}} \rangle_{6,\mathrm{MODEL}}. \tag{3}$$

A_0, the offset term, is a combination of the instrumental uncertainty and unmodeled physics independent of the H_2O absorption. A_1, the slope, shows how well the model can represent the rate at which atmospheric transmission decreases with an increase in H_2O path. The diagonal in Fig. 3 (i.e., $A_0 = 0.0$, $A_1 = 1.0$) indicates perfect agreement. The dashed curve represents the hypothesis that the excess clear-sky absorption of 50% is due solely to H_2O and is proportionally representative in the 0.94 μm region. Using the SIROS MFRSR, A_0 is -0.038, which is small compared to the instrumental uncertainty, and A_1 is 0.950 which indicates excellent agreement when compared to the slope of the dashed curve. (A constant instrumental error of $\pm 5\%$ typical of that identified in a

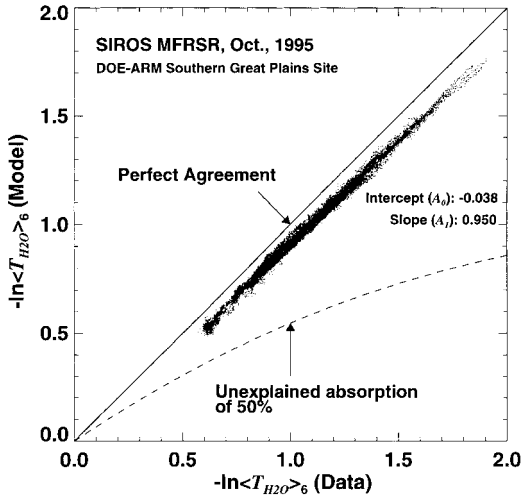

Fig. 3. Scatter plot of $-\ln \langle T_{H_2O} \rangle_{6,\mathrm{MODEL}}$ versus $-\ln \langle T_{H_2O} \rangle_{6,\mathrm{MFRSR}}$. The model 0.94 μm transmission is computed from the correlated-k model of water vapor transmission using vertical profiles of humidity and temperature from the Vaisala sondes and column precipitable water from the microwave radiometer. The observed transmission due to H_2O is from the 0.94 μm channel of the SIROS MFRSR after the effects of Rayleigh scattering and aerosol extinction (inferred simultaneously from the 0.862 μm measurements) have been removed. The diagonal represents perfect agreement, the lower curve represents a 50% unexplained water vapor absorption. Also shown are the offset (A_0) and slope (A_1) of a least-squares linear fit through the data.

Langley calibration, will change A_0 by ± 0.05, but will not change A_1.)

The value of A_1 is independent of differing radiometers, H_2O instruments, sub-sampling techniques, and aerosol optical depths. Using the BSRN MFRSR, A_0 and A_1 both change by only -0.02. When the column H_2O from the MWR is linearly regressed to force agreement with the Vaisala soundings, A_1 does not change. When sub-sampling the data by repeating the analysis for each of the 11 clear-sky days, A_1 varies from 0.90 to 0.97, with a mean of 0.941. This variation is not correlated to day-to-day changes in column H_2O or aerosol optical depth, indicating that the rms variance of 0.02 is not from H_2O or aerosol physics unaccounted for in the models. We test the sensitivity to solar zenith angle by repeating the fitting for eight 0.05 wide solar zenith angle bins from 0.3 to 0.7; A_1 varies from 0.94 to 0.97. There is no apparent trend linking changes in A_1 to zenith angle. Finally, we test the sensitivity to aerosol optical depth by relaxing the assumption that $\tau_{\mathrm{aer},6} = \tau_{\mathrm{aer},5}$. Instead, we let $\tau_{\mathrm{aer},6} = C\tau_{\mathrm{aer},5}$ where C is empirically determined along with A_0 and A_1 using the regression technique (as described above). $C = 1.07$, yielding agreement with our assumption of $C = 1.00$ within the instrumental uncertainty, and A_1 increases by only 0.013. Using aerosol optical depth from channel 2 as the independent variable shows a negligible impact on A_1, validating our single-scattering assumption and aerosol treatment. On the other hand, ignoring the aerosol variability in our determination of $\langle T_{H_2O} \rangle_{6,\mathrm{MFRSR}}$ by replacing $\tau_{\mathrm{aer},6}$ with a constant value of 0.03 causes the slope in Fig. 3 (A_1) to drop from 0.95 to 0.87 — an effect much more pronounced than the other sensitivity studies have produced. Eliminating aerosol altogether produces similar results interchanging the independent and dependent variables in the regression yields a <0.01 change in A_1. Table 1 summarizes the uncertainty in our model-MFRSR agreement.

4. Discussion and conclusion

We next consider the following question: what is the relationship between the model errors at 0.94 μm and the hypothesized broadband (~ 0.2

Table 1. *The sensitivity of A_0 and A_1 to various changes in the analysis method*

	Effect on A_1	Effect on A_0
use of BSRN MFRSR	-0.02	-0.02
day by day fitting	± 0.018 (rms)	± 0.016 (rms)
fixed zenith angle binning	± 0.02	± 0.02
fitting aerosol optical depth (ch. 5)	$+0.01$	0.00
fitting aerosol optical depth (ch. 2)	0.00	-0.01

to 4.0 μm) unmodeled clear-sky H_2O absorption of 25 W m^{-2}? To answer this, we make two points.

- The two independent MFRSRs validate the model H_2O absorption at 0.94 μm to within 5% (Fig. 4). The band at 0.94 μm is typical of the other H_2O vibration-rotation bands in the solar spectrum. If this 5% error were representative of uncertainties in the line parameters of the other strongly absorbing bands, the total broad solar spectrum unexplained absorption due to H_2O would be of order 3 W m^{-2} (globally averaged). This is consistent with the tropical broadband results which allow a maximum 7 W m^{-2} unexplained clear-sky atmospheric absorption.
- The next possibility we explore is that a large, unmodeled continuum absorption (e.g., due to H_2O polymers or non-Voigt line shapes) may be responsible for an unexplained absorption occurring between line centers. This type of absorption is a linear or quadratic function of H_2O, as opposed to the strong-line Voigt absorption modeled here which scales as the square root of H_2O path. If a large continuum absorption were present in the observations, the percent model error found by this study would thus increase with H_2O path. However, we do not see evidence of a strong continuum absorption, either in Fig. 4 (for the 0.94 μm band) or in Figs. 2a, b (for the broadband solar absorption). These results do not necessarily exclude the possibility of a continuum, but they show that it cannot be large enough to explain a 25 W m^{-2} excess absorption in clear skies. (The radiative effects of a near-infrared H_2O continuum is presented in Vogelmann et al., in press.)

Both the tropical broadband data and the Oklahoma spectral data lead us to conclude that the unexplained absorption, if it exists in excess of 7 W m^{-2} (diurnally averaged), is not related to H_2O absorption in clear skies. This finding limits our search for the excess absorption to other (e.g. aerosol or clouds) atmospheric constituents, including H_2O continuum and/or polymer absorption in cloudy skies.

5. Acknowledgements

This work was supported by the Department of Energy Atmospheric Radiation Measurement program grant DE-FG03–91ER61198. We are grateful

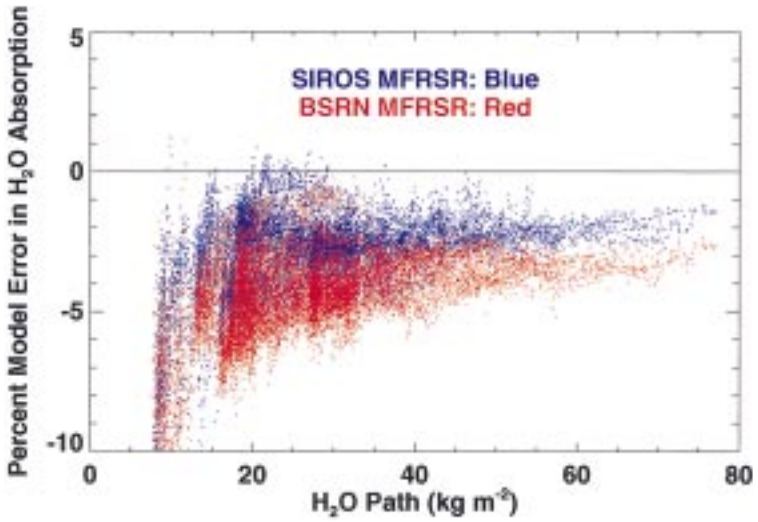

Fig. 4. Percent model error in 0.94 μm water vapor absorption relative to the SIROS (blue) and BSRN (red) measurements plotted versus H_2O path (defined to be vertically integrated column water vapor divided by the cosine of the solar zenith angle). The absorption due to H_2O has been isolated from the measured extinction by removing the effects of Rayleigh scattering, aerosol extinction (inferred directly from the 0.862 μm measurement) and the small A_0 term found to be uncorrelated to water vapor absorption (Fig. 3). The average percent model error determined by the two MFRSRs are −3% for the SIROS, and −4.5% for the BSRN.

to the ARM/SGP and ARM/ARESE teams for access to and interpretation of the ARESE data, and W. Ridgway for the original versions of the line-by-line and correlated-k models used in this study. This is C^4 publication #167.

REFERENCES

Arking, A. 1996. Absorption of solar energy in the atmosphere. Discrepancy between model and observations. *Science* **273**, 779–782.

Blanchet, J.-P. and List, R. 1983. Estimation of optical properties of arctic haze using a numerical model. *Atmosphere-Ocean* **21**, 444–465.

Cess, R. D., Zhang, M. H., Minnis, P., Corsetti, L., Dutton, E. G., Forgan, B. W., Garber, D. P., Gates, W. L., Morcrette, J.-J., Potter, G. L., Ramanathan, V., Subasilar, B., Whitlock, C. H., Young, D. F. and Zhou, Y. 1995. Absorption of solar radiation by clouds: Observations Versus Models. *Science* **267**, 496–499.

Charlock, T. P. and Alberta, T. L. 1996. The CERES/ARM/GEWEX Experiment (CAGEX) for the retrieval of radiative fluxes with satellite data. *Bull. Am. Met. Soc.* **77**, 2673–2683.

Chou, M.-D. and Zhao, W. 1997. Estimation and model validation of surface solar radiation and cloud radiative forcing using TOGA COARE measurements. *J. Clim.* **10**, 610–620.

Conant, W. C. 1996. *An examination of the solar absorption under clear skies for the central equatorial Pacific. Observations versus models.* MS thesis, University of California, 50 pp.

Conant, W. C., Ramanathan, V., Valero, F. P. J. and Meywerk, J. 1997. An examination of the clear-sky solar absorption over the central equatorial pacific: observations versus models. *J. Climate* **10**, 1874–1884.

Harrison, L. C. and Michalsky, J. J. 1994. Objective algorithms for the retrieval of optical depths from ground-based measurements. *Appl. Optics* **33**, 5126–5132.

Harrison, L. C., Michalsky, J. J. and Berndt, J. 1994. Automated multifilter rotating shadow-band radiometer. An instrument for optical depth and radiation measurements. *Appl. Optics* **33**, 5118–5125.

Kiehl, J. T. and Trenberth, K. E. 1997. Earth's annual global mean energy budget. *Bull. Am. Meteorol. Soc.* **78**, 197–208.

Lacis, A. A. and Oinas, V. 1991. A description of the correlated-k distribution method for modeling nongray gaseous absorption, thermal emission, and multiple scattering in vertically inhomogeneous atmospheres. *J. Geophys. Res.* **96**, 9027–9063.

Li, Z., Leighton, H. G., Masuda, K. and Takashima, T. 1993. Estimation of SW flux absorbed at the surface from TOA reflected flux. *J. Clim.* **6**, 317–330.

Liljegren, J. C. 1994. Two-channel microwave radiometer for observations of total column precipitable water vapor and cloud liquid water path. *5th Symposium on Global Change Studies*, 262–269.

Liou, K. N. 1992. *Radiation and cloud processes in the atmosphere*, Oxford Press.

Michalsky, J. J., Liljegren, J. C. and Harrison, L. C. 1995. A comparison of Sun photometer derivations of total column waver vapor and ozone to standard measures of same at the Southern Great Plains atmospheric radiation measurement site. *J. Geophys. Res.* **100**, 25,995–26,003.

Ohmura, A. and Gilgen, H. 1993. Re-evaluation of the global energy balance. *Geophys. Monogr.* no. 75, IUGG, 93–110.

Pilewskie, P. and Valero, F. P. J. 1995. Direct observations of excess solar absorption by clouds. *Science* **267**, 1626–1628.

Ramanathan, V., Subasilar, B., Zhang, G. J., Conant, W. C., Cess, R. D., Kiehl, J. T., Grassl, H. and Shi, L. 1995. Warm pool heat budget and shortwave cloud forcing: A missing physics? *Science* **267**, 499–503.

Rothman, L. S., Gamache, R. R., Tipping, R. H., Rinsland, C. P., Smith, M. A. H., Benner, D. C., Devi, V. M., Flaud, J.-M., Camy-Peyret, C., Perrin, A., Goldman, A., Massie, S. T., Brown, L. R. and Toth, R. A. 1992. The HITRAN molecular database: Editions of 1991 and 1992. *J. Quant. Spectrosc. Rad. Trans.* **48**, 469–507.

Stephens, G. L. 1996. How much solar radiation do clouds absorb? *Science* **271**, 1131–1134.

Teillet, P. M. 1990. Rayleigh optical depth comparisons from various sources. *Appl. Optics* **29**, 1897–1900.

Valero, F. P. J., Schwartz, S. E., Cess, R. D., Ramanathan, V., Minnis, P., Ackerman, T. P. and Tooman, T. P. 1995. *ARESE* (*ARM Enhanced Shortwave Experiment*) Science Plan. Available from the United States Department of Energy, 53 pp.

Vogelmann, A. M., Ramanathan, V., Conant, W. C. and Hunter, W. E. 1997. Observational constraints on the non-lorentzian continuum effects in the near-infrared solar spectrum using ARM ARESE data. *J. Quant. Spectrosc. Rad. Trans.*, in press.

Waliser, D. E., Collins, W. D. and Anderson, S. P. 1996. An estimate of the surface shortwave cloud forcing over the western Pacific during TOGA COARE. *Geophys. Res. Lett.* **23**, 519–522.

Wild, M., Ohmura, A., Gilgen, H. and Roeckner, E. 1995. Validation of general circulation model radiative fluxes using surface observations. *J. Clim.* **8**, 1309–1324.